

Distribution network capability as a limiting factor of wind power plant connection

N. Dizdarevic, M. Majstrovic, *Member, IEEE*, and L. Horvath

Abstract – Lack of sufficient distribution network capability is seen in this paper as a limiting factor of wind power plant (WPP) installation. The problem is viewed from time domain responses of the WPP to wind speed changes. Being disturbed by a variable wind speed, the WPP injects variable active and reactive power into the distribution network exposing nearby consumers to excessive voltage changes. The WPP connection is analyzed with respect to line thermal limits, bus voltage fluctuations and network power loss. Potential electrical energy production of a real WPP installation site is related to surrounding distribution network capability. Recognized discrepancy pointed out to a necessity of application of further countermeasures should this installation site be made viable for full utilization.

Index Terms - distribution network capability, thermal loading, voltage fluctuation, power loss, wind power plant (WPP)

I. INTRODUCTION

Alternative solutions treating distributed generation have appeared as a consequence of strong ecological concerns with regard to almost all major industrial branches [1]-[3]. Initiatives of potential investors come along with liberalization of electricity market providing an additional impact to a need for conducting a new kind of technical analysis [4]-[5]. Grid integration aspects of renewable sources have become increasingly important as incentives come in large numbers [6]-[7]. From distribution network viewpoint, connection of small wind power plants calls for urgent attention.

Increased penetration of wind energy creates an uncontrollable component in power system. Dynamic changes of wind speed make amount of power injected to a network highly variable. Depending on intensity and rate of changes, difficulties with thermal loadings, voltage fluctuations and power loss could appear. Conditions of economic justification set project requirements for wind power plant installations in areas with high wind utilization. Such areas are often located in rural zones with relatively weak electrical networks.

From that viewpoint, the objective of this paper is set as to point out to a discrepancy that arises between potential electrical energy production of a real installation site and surrounding distribution network capability. That discrepancy could be so large that without an adequate countermeasure only a small number of windturbines may be connected due to weak voltage conditions and increased network loss. That would not only leave assessed wind potential unused, but it could also prohibit installation of larger number of wind turbines jeopardizing the economics of the whole project.

N. Dizdarevic is with the Energy Institute “Hrvoje Pozar”, Zagreb, Croatia (e-mail: ndizdar@eihp.hr; web: www.eihp.hr/~ndizdar).

M. Majstrovic is with the Faculty of Electrical Engineering, University of Split, Croatia (e-mail: matislav@fesb.hr).

L. Horvath is with the Energy Institute “Hrvoje Pozar”, Zagreb, Croatia (e-mail: lhovath@eihp.hr).

II. SITE POTENTIAL OF ENERGY PRODUCTION

The installation site called 'Stupisce' is located at south-west part of the island Vis (Adriatic Sea), Republic of Croatia, at a distance of 4 km from town Komiza [8]. The site is a plain of size 2000 m by 700 m at an altitude level between 150 m and 200 m above sea. It gradually decreases towards open sea waters. The rocky terrain is covered with low bushes and mostly subjected to south-east wind. Nearby, there is an approaching road and a 10 kV overhead line (820 m).

At the site, wind speed is measured since May 1996 [9]. Estimated parameters of Weibull distribution (A and k) and a yearly average wind speed (v) at four different heights from the soil (10, 25, 50 and 100 m) are shown in Table 1. Probability of wind speed being larger than 3 m/s, 5 m/s, 7 m/s and 10 m/s at these heights are given in Table 2.

Table 1. Yearly average wind speed (v) at four heights

Heights above soil (m)	Weibull parameter A (m/s)	Weibull parameter k	Yearly mean Wind speed v (m/s)
10	7.4	1.44	6.7
25	7.9	1.57	7.1
50	8.4	1.77	7.5
100	9.0	1.95	8.0

Table 2. Probability of larger wind speeds at four heights

Heights above soil (m)	Probability (%)			
	3 m/s	5 m/s	7 m/s	10 m/s
10	77.5	57.2	39.4	20.5
25	81.6	62.0	43.2	22.1
50	86.0	67.7	48.1	24.3
100	89.9	73.9	54.6	28.6

Computation of natural and technical potential of electrical energy production from wind energy at the site is conducted by using the same streaming model [10]. Three different kinds of windturbines are selected at first, followed by estimation of their potential for energy production (Table 3). Windturbines are selected as typical representatives of solutions and developmental directions in wind technology. Number of windturbines at the site is defined by their sizes. Distance between each other is restricted to at least 5 rotor diameters.

Gross electrical energy production at the site is between 18.5 GWh and 28.2 GWh per year [9]. Chosen windturbines have between 2,300 and 2,656 operation hours per year, which counts for 26.2% and 30.3% respectively. Productivity per rotor swept area is between 946 and 1,021 kWh/m². In the worst case, the WPP have 6.8 MW of total installed power. The WPP should be connected to a nearby 10 kV overhead line (820 m). Thus, in the next step of the feasibility analysis it is necessary to check out whether it is possible to evacuate power from the WPP regarding technical characteristics of a distribution network to which it should be connected.

Table 3. Site potential for electrical energy production from wind energy depending on windturbines technology

Characteristics of windturbines	Windturbines		
	1	2	3
Nominal power (kW)	1,500	850	750
Rotor diameter (m)	70.5	52	48.2
Tower height (m)	64.5	55	55
Nominal speed (m/s)	13	14	13
Power regulation	pitch	pitch	stall
Number of installed windturbines	6	9	9
Installed power (MW)	9.0	7.7	6.8
Gross production (MWh)	28,182	22,518	18,535
Operation hours (MWh/MW)	2,656	2,453	2,300
Productivity (kWh/m ²)	1,021	982	946

III. SYSTEM MODELLING

Feasibility of the WPP power evacuation through a distribution network is set here as the main objective. The WPP is connected to the 10 kV distribution network (78 buses, 77 branches) with no other generating units except the one at the main in-feed point representing a slack bus at 110 kV (Fig. 1). The 10 kV distribution network is connected through 10 kV /35 kV transformers to the 35 kV network, and further on to the 110 kV transmission network. Total length of 35 kV paths equals 43.6 km. The length of the 10 kV radial feeder to which the WPP is connected equals 15.6 km. Short circuit power at the bus TS Starigrad 110 kV is equal to $S_{K35}=1103$ MVA ($I_{K35}''=5788\angle-69.1^\circ$ A, $Z_{th}=10.97 \Omega$). Total maximum load of the 10 kV network is equal to 3.2 MW/0.989 Mvar. Basic parameters of the system are given in the Appendix.

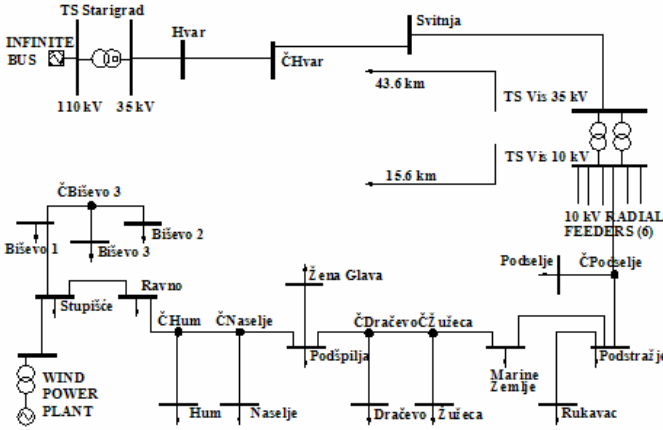


Fig. 1. Distribution network with embedded wind power plant

IV. THE WPP MATHEMATICAL MODEL

The analysis is conducted by using in-house developed and programmed combined dynamic and static model. It is supposed that the WPP is of a fixed speed/constant frequency type that is equipped with an induction generator driven by an unregulated wind turbine [11-13]. If such a system is connected to a weak network, some fast and large changes around a mean wind speed may cause excessive voltage changes to nearby consumers due to fluctuations in the WPP injected power. Differential equation describing dynamics of induction generator transient model is

$$\frac{d\bar{E}'_{gen}}{dt} = -j\omega_{0s} s \bar{E}'_{gen} - \frac{1}{T_0} \left[\bar{E}'_{gen} + j(X - X') \bar{I}_{gen} \right], \quad (1)$$

where reactance X and time constant T_0' are obtained from

$$X = X_s + X_{mag}, \quad (2)$$

$$T_0' = \frac{X_r + X_{mag}}{\omega_{0s} R_r}. \quad (3)$$

After d-q decomposition, eq. (1) becomes

$$\frac{dE'_q}{dt} = (\omega_{0s} - \omega_m) E'_d - \frac{E'_q}{T_0'} + \frac{X - X'}{T_0'} I_d, \quad (4)$$

$$\frac{dE'_d}{dt} = -(\omega_{0s} - \omega_m) E'_q - \frac{E'_d}{T_0'} - \frac{X - X'}{T_0'} I_q. \quad (5)$$

Electromechanical dynamics of two-mass shaft is defined by

$$\frac{d\Theta_c}{dt} = \omega_T - \frac{\omega_m}{n}, \quad (6)$$

$$\frac{d\omega_T}{dt} = \frac{\frac{P_w(V_w)}{\omega_T} \frac{1}{S_{ngen}} - c_c \Theta_c - (D_c + D_T) \omega_T + \frac{D_c}{n} \omega_m}{2H_T}, \quad (7)$$

$$\frac{d\omega_m}{dt} = \frac{\frac{c_c}{n} \Theta_c + \frac{D_c}{n} \omega_T - \left(D_m + \frac{D_c + D_g}{n^2} \right) \omega_m - T_e}{2 \left(H_m + \frac{H_g}{n^2} \right)}, \quad (8)$$

where is

- Θ_c shaft torsion angle between wind turbine and induction generator rotor (rad_c),
- ω_T, ω_m wind turbine and induction generator rotor speeds (pu values, in steady state $\omega_T = \omega_m/n$),
- $l:n$ transmission gear ratio between two speeds,
- P_w aerodynamic power (W),
- V_w wind speed (m/s),
- S_{ngen} rated apparent power of ind. generator (VA),
- c_c torsion stiffness coefficient (pu/rad_c),
- D_c torsion damping coefficient (pu/pu),
- D_T damping coefficient of wind turbine (pu/pu),
- D_g damping coefficient of gear-box (pu/pu),
- D_m damping coefficient of ind. generator (pu/pu),
- H_T inertia constant of wind turbine (s),
- H_g inertia constant of gear-box (s), and
- H_m inertia constant of induction generator (s).

The electromagnetic torque T_e is computed as it follows

$$T_e = (E'_d I_d + E'_q I_q) / \omega_{0s}. \quad (9)$$

Besides differential equations, the transient model of induction generator comprises four algebraic equations

$$-X' E'_q + R_s E'_d - (R_s^2 + X'^2) I_d - R_s V_d + X' V_q = 0, \quad (10)$$

$$R_s E'_q + X' E'_d - (R_s^2 + X'^2) I_q - X' V_d - R_s V_q = 0, \quad (11)$$

$$V_d - V_n \sin \Theta_n = 0, \quad (12)$$

$$V_q - V_n \cos \Theta_n = 0. \quad (13)$$

By changing wind speed V_w it is made possible to compute time-domain responses of the WPP variables.

V. NUMERICAL RESULTS

Feasibility of the WPP power evacuation through the distribution network is analyzed within a scope of line thermal loadings, bus voltage fluctuations and power loss problem as a part of the technical aspects of grid integration of the WPP.

In the following part, study results are given for the basic configuration of the 10 kV distribution network and for one that is optionally reinforced to help solve detected weaknesses. The reinforcements are introduced by building new 10 kV underground cable (3 km) and upgrading short section of an overhead line (150 m). At the WPP connection bus (Stupisce), three-phase short-circuit power is 3 times greater in the reinforced configuration than in the basic one (Table 4).

Table 4. Short-circuit capacity at the WPP connection point

VARIANT	BUS	U	I" k3	S" k3	Z	ang [°]	R/X
BASIC	STUPIŠČE	10kV	0.91kA	15.8MVA	6.9Ω	58.8	0.61
REINFORCED	STUPIŠČE	10kV	2.74kA	47.5MVA	2.3Ω	71.0	0.34

The potential power of the site is checked against network thermal loadability at first. Then, a maximum number of windturbines is computed with respect to power conditions at network buses seen as functions of wind speed changes.

Based on network capability criteria, in radial distribution network the maximum installed power of the WPP depends on transfer capability of the most critical section between the WPP and an infinite bus. In the basic configuration, thermal loading of the 10 kV radial feeder is limited by a critical section to 160 A (2.771 MVA), while in the reinforced one to 360 A (6.062 MVA). Since in this analysis nominal apparent power of one fully compensated windturbine is equal to 0.803 MVA, in the basic configuration it makes possible to connect 3 windturbines, and in the reinforced one 7 windturbines. This conclusion should be checked with respect to voltage fluctuations as well. In addition to active power injection, voltage fluctuations are also related to reactive power compensation. When switching capacitor banks on, generator voltage is increased and that voltage change is transferred further on through the network. The point of the WPP network connection is often located electrically far from the main in-feed point. Then, voltage fluctuations could be so excessive that they limit number of installed windturbines at the site even though the network thermal loadability is sufficient.

In order to pass through a full-scale range of the windturbines operating values $P_w(V_w)$ (Fig. 2), a slow linear change of wind speed V_w is applied from 4 m/s (cut-in) to 25 m/s (cut-out) during 1400 s. This change enables windturbine to inject active power from minimum to maximum value in a manner slow enough not to induce unwanted oscillations.

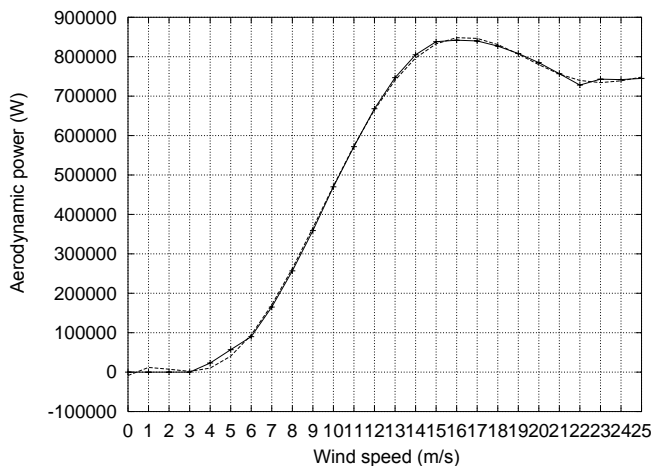


Fig. 2. Windturbine $P_w(V_w)$ curve

All computations are conducted within continuous operation of the WPP. Induction generator is viewed as a reactive power consumer, which consumption depends on active power production. Shunt capacitor banks are connected at the generator terminals (8x50 kvar), and automatically switched on/off if generator reactive power exceeds ± 30 kvar for longer than 15 s. Each generator is equipped with two sets of stator windings that belong to smaller/larger rating powers (g/G). Its switching happens at the wind speed of 7.335 m/s.

During linear change of wind speed, the injected active power P_{egen} becomes variable according to the $P_w(V_w)$ curve, while causing change in reactive power that induction generator simultaneously draws from the network (Fig.3). At the network connection point, the WECS should inject active power with minimum exchange of reactive one. As a conventional countermeasure, capacitor banks are switched on/off in a generator bus to keep generator reactive power exchange within predefined boundaries of ± 30 kvar (Fig. 4).

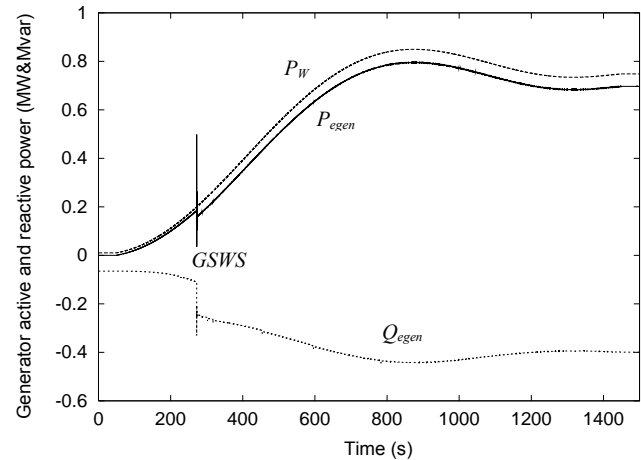


Fig. 3. Active and reactive power of induction generator

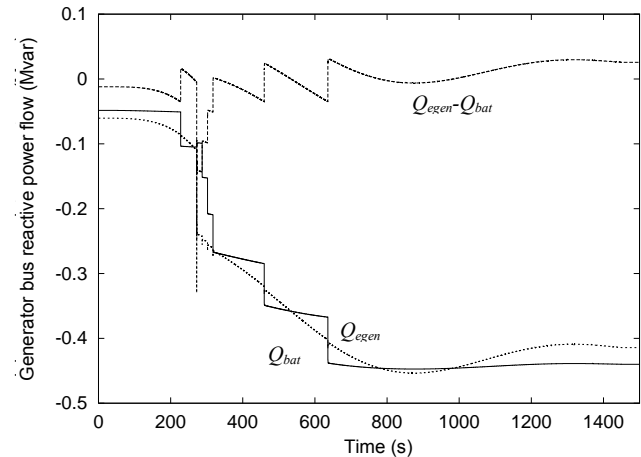


Fig. 4. Reactive power flow in generator bus

If only two such windturbines are connected in the basic configuration of the network, excessive voltage fluctuations appear and limit full utilization of the site potential. Unused thermal loading margin is significant (around 50%). However, increased number of the windturbines at the site in the basic configuration makes that thermal loading margin utilized, but bus voltage magnitudes become unacceptably high (Figs. 5-6). Obvious limiting factor here is small voltage stiffness at the point of the WPP connection.

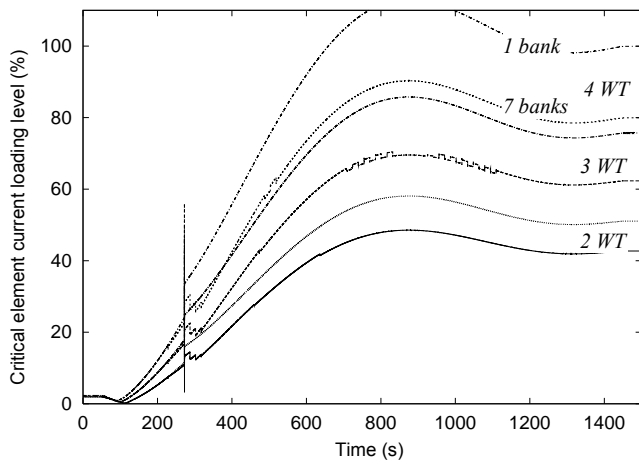


Fig. 5. Critical current loading level along 10 kV radial feeder

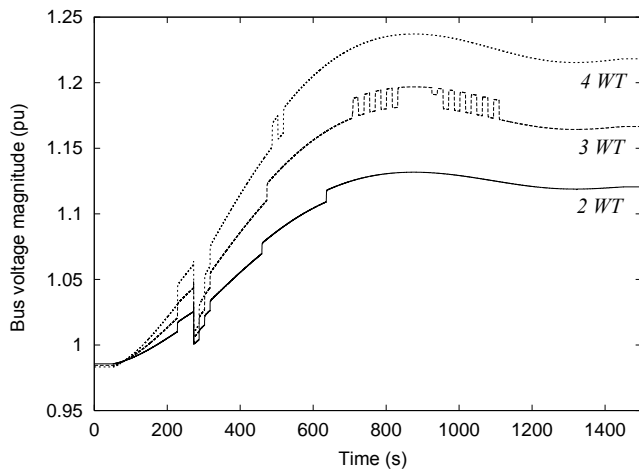


Fig. 6. Bus voltage magnitude at the point of the WPP connection

Increased number of windturbines makes large impact to power loss in the basic configuration of the 10 kV network (Fig. 7). With 4 windturbines, power loss is almost 4 times greater than that with 2 windturbines, and 2 times greater than that with 3 windturbines. Full reactive compensation with 7 capacitor banks at each induction generator decreases active power loss due to smaller reactive power flow through the radial feeder. In comparison to the starting state which is close to the situation without the WPP connected to the network, power loss becomes increased with intensified operation.

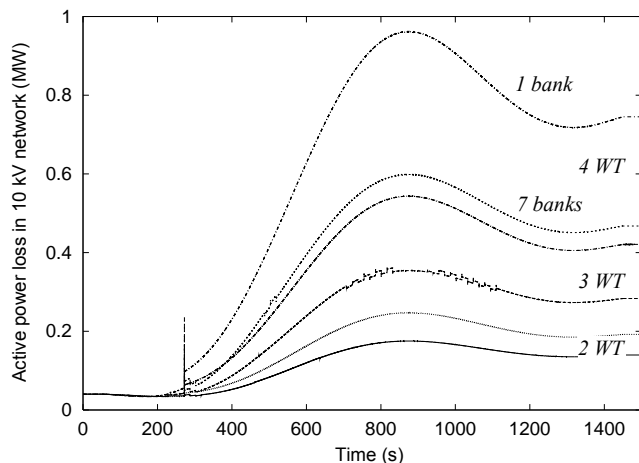


Fig. 7. Active power loss in the 10 kV network

The reinforced configuration is established to accommodate at least 7 windturbines at the same site. Bus voltage magnitude at the WPP connection shows that network reinforcements enabled installation with 7 windturbines to cause voltage situation similar to the basic case with two windturbines (Fig. 8). By using 6 capacitor banks, the largest bus voltage magnitude is equal to 1.095 pu (+11%). With full compensation (7 banks), it rises to 1.12 pu (+14%) and enters in the area of continuous switching on/off of the highest bank. This area appears when generator voltage becomes larger than the critical value with respect to tolerance zone (1.096 pu vs. ± 30 kvar). If the 7th bank (50 kvar) is switched on at the critical voltage, then the tolerance zone is jumped over from below minimum (-30 kvar) to above maximum (+30 kvar), and vice versa. Current loading level in the reinforced network with 7 windturbines does not cross over 80% of thermal limit (Fig. 9). Provided better voltage situation, it might be possible to accommodate here even larger number of windturbines.

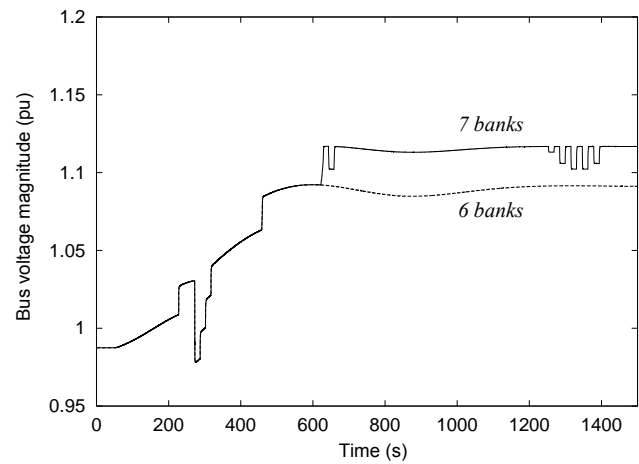


Fig. 8. Bus voltage magnitude at the point of the WPP connection - reinforced configuration, 7 windturbines -

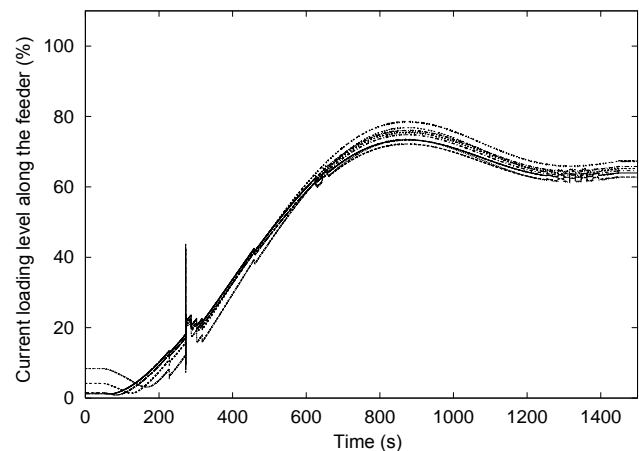


Fig. 9. Current loading level along 10 kV radial feeder - reinforced configuration, 7 windturbines -

Number of installed windturbines (7, 8 or 9) at the site within reinforced configuration is limited with respect to the bus voltage magnitude at the point of the WPP connection (Fig. 10). Only in the case with 7 installed windturbines, the voltage situation could be considered as acceptable. In two other cases, voltage fluctuations are excessive. Current loading level does not represent here a limiting factor (Fig. 11).

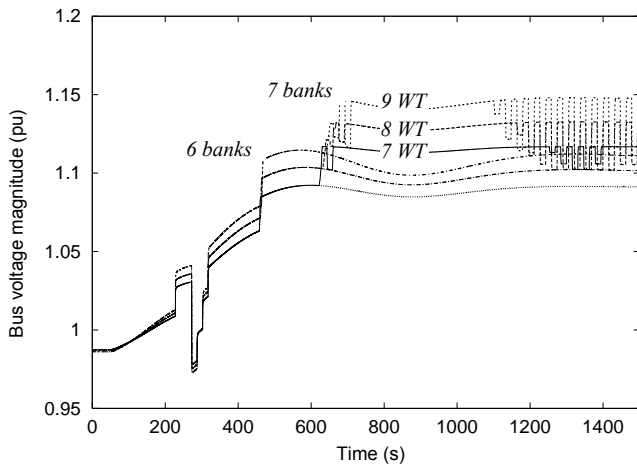


Fig. 10. Bus voltage magnitude at the point of the WPP connection - reinforced configuration, 7 windturbines -

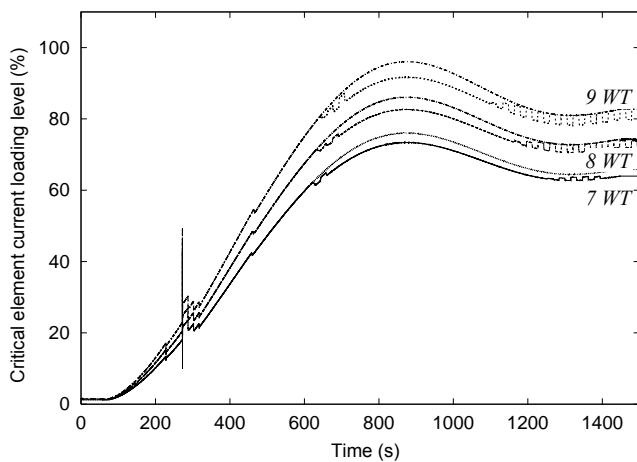


Fig. 11. Current loading level along 10 kV radial feeder - reinforced configuration, 7 windturbines -

Number of installed windturbines makes significant impact to active power loss in the 10 kV reinforced distribution network (Fig. 12). In situation with 9 windturbines, power loss is 70% larger than that with 7 windturbines. When having installed 7 windturbines, power loss is approximately equal to $\frac{1}{2}$ of nominal power of one windturbine. When having installed 9 windturbines, power loss is almost equal to the nominal power of one windturbine.

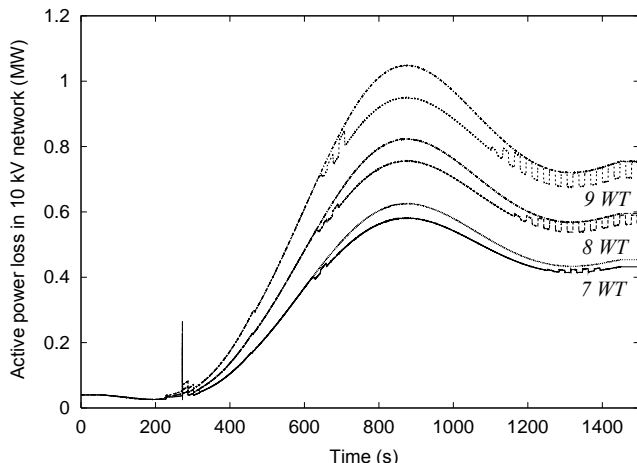


Fig. 12. Active power loss in the 10 kV network - reinforced network, 7 windturbines -

Power conditions in basic and reinforced configurations are hereafter dynamically analyzed as functions of measured wind speed changes at the site and of measured active and reactive load power in the network during 48-hour period [13]. Total amounts of the load power are measured at the 10 kV in-feed point of the distribution network, and distributed over 10 kV network load buses in proportion to their maximum loadings. The load power represents average value of each 10-minute interval during 48-hour period. The constant minimum (4 m/s), constant maximum (16 m/s) and intermittent operating regimes in terms of variable WPP wind speed are superimposed to simultaneously variable bus load power in order to estimate severity of network operation. The intermittent wind speed pattern is taken as an average value of each 10-minute interval between 4 m/s and 25 m/s. The WPP operation is without start-up and shut-down discontinuities.

Injected power of the WPP is variable with respect to the superimposed changes. Excessive voltage fluctuations appear in the basic configuration with 2 windturbines installed. Bus voltage magnitude at the WPP connection depicts low voltage stiffness (Fig. 13). The reinforcements enabled installation of 7 windturbines to cause similar voltage situation (Fig. 14).

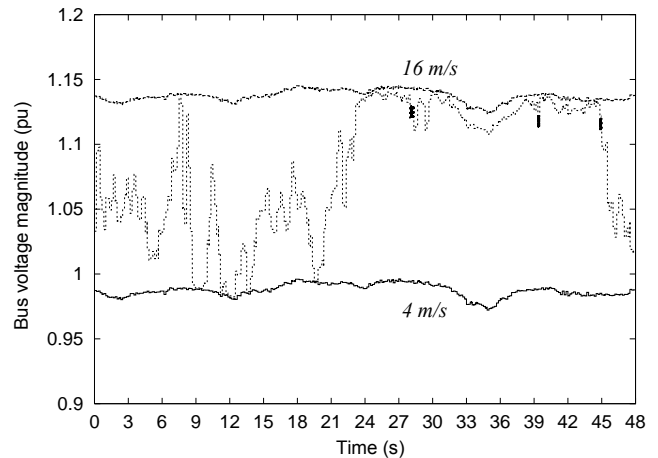


Fig. 13. Bus voltage magnitude at the point of the WPP connection - basic configuration, 2 windturbines -

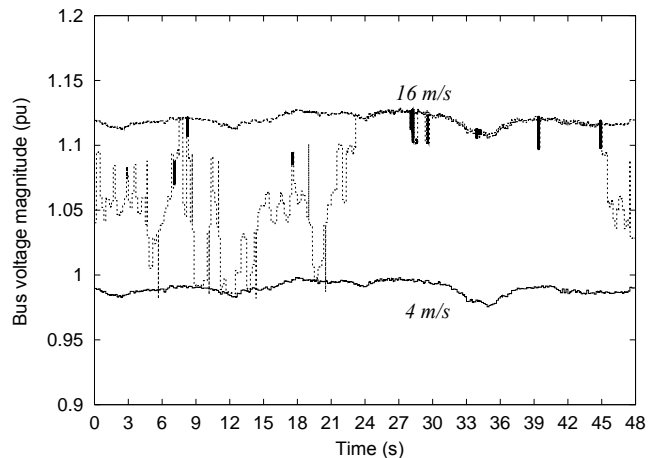


Fig. 14. Bus voltage magnitude at the point of the WPP connection - reinforced configuration, 7 windturbines -

Active power loss in the basic network configuration with 2 windturbines installed (Fig. 15) is lower than that in the reinforced configuration with 7 windturbines (Fig. 16).

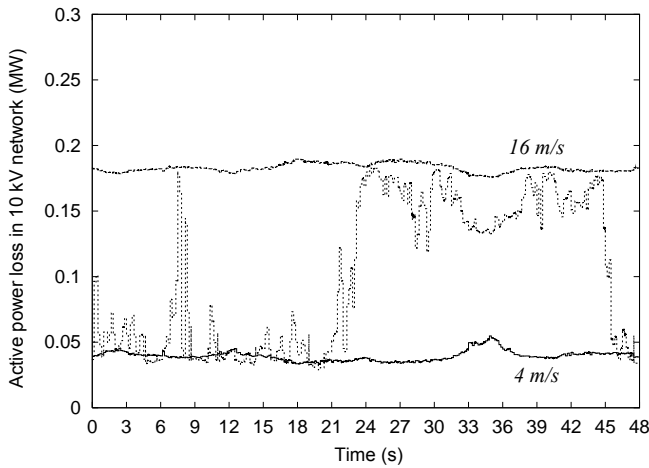


Fig. 15. Active power loss in the 10 kV network - basic network, 2 windturbines -

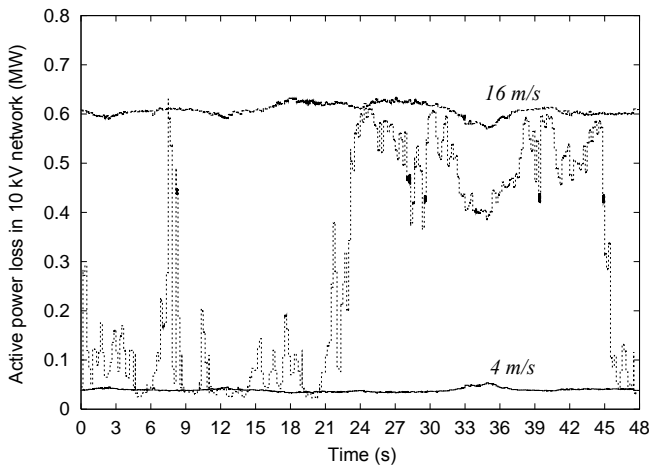


Fig. 16. Active power loss in the 10 kV network - reinforced network, 7 windturbines -

VI. CONCLUSIONS

Maximum number of windturbines is computed with respect to thermal loadings, voltage fluctuations and power loss in the 10 kV distribution network. It is related to potential electrical energy production from wind energy at the site. Utilization of the site potential could be made viable only upon serious network reinforcement or any other countermeasure. Without an adequate countermeasure, only a small number of windturbines may be connected due to weak voltage conditions and increased power loss. That would not only leave assessed wind potential unused, but it could also prohibit installation of larger number of wind turbines jeopardizing the economics of the whole project.

VII. REFERENCES

- [1] N. Jenkins et al., *Embedded generation*, IEE Power and Energy Series 31, ISBN 0 85296 774 8, London, UK, 2000
- [2] CIGRÉ, *Impact of increasing contribution of dispersed generation on the power system*, WG 37.23, Feb. 1999
- [3] T. Ackermann et al., "Distributed generation: a definition", *Electric Power Systems Research*, vol. 57, 2001, pp. 195-204
- [4] N. Hatzigiorgiou, "Distributed energy sources: Technical challenges", *IEEE 2002 Winter Meeting*, NY, USA, Jan. 2002

- [5] J. Lopes, "Integration of dispersed generation on distribution network – Impact studies", *IEEE 2002 Winter Meeting*, NY, USA, Jan. 2002
- [6] S. Heier, *Grid integration of wind energy conversion systems*, John Wiley & Sons, 1998
- [7] CIGRÉ, *Modelling new forms of generation and storage*, WG 38.01, Nov. 2000
- [8] Horvath, L. et al., "ENWIND – Programme of wind energy using: Previous results and future activities", Energy Institute "Hrvoje Pozar", Zagreb, Croatia, April 1998
- [9] Horvath, L. et al., "ENWIND – Programme of wind energy using: New findings and realization", Energy Institute "Hrvoje Pozar", Zagreb, December 2001
- [10] WA²P - Wind Atlas Analysis and Application Programme, Risø National Laboratory, Denmark
- [11] N. Dizdarevic, M. Majstrovic, S. Zutobradic, D. Bajs, *Grid integration of wind energy conversion system*, project study for Croatian Electric Company, Energy Institute HRVOJE POZAR, Zagreb, Croatia, February 2003, [Online]. Available: www.eihp.hr/~ndizdar
- [12] N. Dizdarevic, M. Majstrovic, and G. Andersson, "FACTS-based reactive power compensation of wind energy conversion system", *Proceedings of the 2003 IEEE Bologna PowerTech*, Bologna, Italy, June 2003, Paper BPT03-251, [Online]. Available: www.eihp.hr/~ndizdar
- [13] N. Dizdarevic, M. Majstrovic, and G. Andersson, "Longer term stabilisation of wind power plant voltage/reactive power fluctuations by FACTS solution," *Proceedings of the IASTED Power and Energy Conference EuroPES 2003*, Marbella, Spain, September 2003, Paper 409-117, [Online]. Available: www.eihp.hr/~ndizdar

VIII. BIOGRAPHIES

Nijaz Dizdarevic received his B.S., M.S., and Ph.D. degrees from Univ. Zagreb, Croatia, in 1990, 1994, and 2001, respectively. From 1991 till 2001 he was with the Dept. Power Systems at the same Faculty. During 1996 and 1997 he was at the KTH Stockholm, Sweden. Since 2002 he is with the Energy Institute "H. Pozar", Zagreb, working on power system stability.

Matslav Majstrovic received his B.S., M.S., and Ph.D. degrees from Univ. Split and Univ. Zagreb, Croatia, in 1973, 1979, and 1986, respectively. He is currently a senior researcher at the Energy Institute "H. Pozar" Zagreb and a full professor at the University of Split, Faculty of Electrical Engineering in the area of electricity transmission and distribution network analysis.

Laszlo Horvath received his B.S., degree from Univ. Zagreb, Croatia, in 1994. From 1995 he is with the Energy Institute "H. Pozar", Zagreb, working on wind power utilization.

IX. APPENDIX

Table A.1 The WPP rated values (G/g)

P_n (kW)	7x(800/200)
U_n (V)	690 V \pm 10 %
S_n (kVA)	909/232
$I:n$	1:63.6
R_s (Ω)	0.0131/0.1165
X_s (Ω)	0.24/0.72
R_r (Ω)	0.014/0.073
X_r (Ω)	0.16/0.97
X_{max} (Ω)	5.94/22.2
H_m (s)	0.234/0.410
H_g (s)	0.008/0.014
H_T (s)	5.644/9.787
θ_c ($^\circ$)	3.6 $^\circ$ /3.6 $^\circ$
c_c (pu torque/rad $_e$)	884/821
D_c (pu torque/pu speed)	1200/1200
D_m (pu torque/pu speed)	0.008664/0.008031
D_g (pu torque/pu speed)	1.168/1.083
D_T (pu torque/pu speed)	147.15/136.73